http://ansinet.com/itj

ITJ

ISSN 1812-5638

INFORMATION TECHNOLOGY JOURNAL

ANSInet
Asian Network for Scientific Information
308 Lasani Town, Sargodha Road, Faisalabad - Pakistan

Information Technology Journal 7 (7): 1001-1008, 2008
ISSN 1812-5638

The Research on Control of Lunar Rover with Rocker Bogie Based on Bus Network Driving

X. Yu, H. Gao and Z. Deng
School of Mechatronics Engineering, Harbin Institute of Technology, Harbin 150001, China

Abstract: This research analysis mechanism of multi-wheel corresponding driven and steady driven of lunar rover with 6 wheels and rocker bogie based on its characterization of mechanical configuration and based on principle of traditional multi-wheels driven, using the CAN bus, we construct a distributed motion control network as a kernel of whole control system of rover. The bus network motion control unit adopts uniform interface, uniform hardware body and this unit has characteristics of modularization, easy to reconfiguration and high integration. The distributed motion control system based on this unit can decrease the complexity of wiring of robot and improve flexibility of programming of main computer of rover. Using wheel operation modes, motion performance of rover is analyzed in 3 different driving modes on smooth and rough terrain. According to the mechanical configuration of rover, operations modes of wheel and principle of speed matching of wheels, we presents a adaptive coordinated control algorithm of multi-wheels independent driven on rough terrain. Through the experiments of obstacle overcoming, climbing, moving on cross-hill in soft soil and spot turning, it shows this rover has good transportation performance, the distributed motion control system base CAN bus has a good performance and high reliability and the adaptive coordinated control algorithm is validity.

Key words: Lunar rover, multi-wheels coordinated control, bus network driving, distributed motion control, modularization

INTRODUCTION

Multi-wheels driving is a study focus in rover control; its mechanism is related with structure and configuration of rover. Traditional driving mode usually adopts centralized control, only one computer does all tasks and control algorithm of system (Schenker *et al*., 2001; Iagnemma *et al*., 1999; Matijevic and Shirley, 1997; Nesnas *et al*., 2003). But this mode has many disadvantages including overload of main system, high fault rate, short-lived, connecting more and safeguard hard etc. Now distributed mode has been adopted in motion control of planetary rover. This mode uses field bus to connect all drivers and other components. Tsinghua University prototype of lunar rover adopts EIA-RS485 to connect all driving and steering wheels (Lin *et al*., 2000) and Rocky 8 and K9 of JPL also use distributed motion mode (Nesnas *et al*., 2003; Volpe *et al*., 2001): Rocky 8 uses I^2C for all motion drivers and K9 uses RS422. A key of distributed motion control is synchronization of command implementing for all drivers. It includes software and hardware synchronization. K9 supports hardware synchronization, but Rocky 8 does not. This rover with rocky-bogie has 8 driving wheels, 4 steering wheels and many sensors, in order to simple interface, CAN bus is adopted. It has advantages of high reliability, far transmission distance and stronger fault tolerant and supporting hardware synchronization. A servo motion driver is constructed, which has characteristics of rapidity, stability and higher precision (Chen *et al*., 2006) and can realize adaptive control algorithm according to different motion states. Through CAN bus and high precision servo motion, it is easy to complete multi-wheel independent driving for rover. This study presents motion control system based on bus network driving and designs servo motion driver based on CAN bus. On this basis, it is analyzed different driving mode has different effect on motion performance of rover. At last, according to configuration of rover, a modified algorithm is presented to improve performance of rover in rough terrain.

COMPONENTS OF ROVER WITH ROCKER BOGIE

The components of rover with rocker-bogie are shown in Fig. 1. It is designed based on environment of

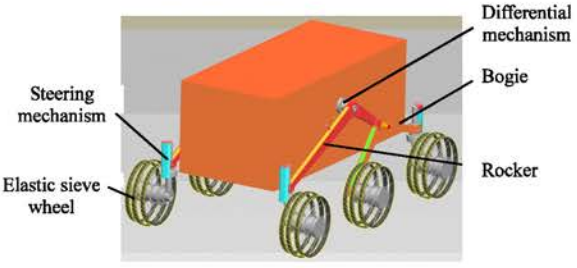

Fig. 1: Prototype CAD model of lunar rover with rocker-bogie

Corresponding Author: Xinyi Yu, School of Mechatronics Engineering, Harbin Institute of Technology, Harbin, 150001, China

moon and modularization. Its configuration has characteristics of good performance with passive adaptation for the terrain, stronger climbing obstacle capability and stability. Its chassis is composed of suspension base with 2 rocker-bogie and differential mechanism. Each rocker-bogie has 3 independent driven wheels and 2 steering wheels.

Elastic sieve wheel is adopted to improve transport performance in soft terrain. It reduces vibration induced by rigidity wheel and increases stationary of rover moving in rough terrain.

DESIGN OF NETWORK WITH DISTRIBUTED DRIVING BASED ON CAN BUS

Structure of distributed driving based on CAN bus: Distributed control system is adopted in control of rover; it has characteristics of modularization, reconfiguration and extensibility. Its structure of distributed network control diagram of rover control system is shown in Fig. 2. Rover control system is designed according to basic control elements and motor driver uses same control module. Configuration of each control module includes driver unit of 2 motor, 8 channel analog input, 8 channel digital outputs and 8 channel digital inputs. Parameters such as PID parameter and control mode can be configured by software.

The key is how to solve command synchronization for multi-wheels driven based on bus networking. It can generally be divided into two kinds: Software and hardware synchronization. CAN bus is broadcasting form networks, so it can realize hardware synchronization. Using this advantage of CAN bus, it is guaranteed that command implementing is synchronization for multi-wheels coordinated control of rover.

The flow process of chart of software of locomotion subsystem is shown in Fig. 3. Its characteristics are followed as:

- Reliability, the program should be robust and the defined function module should be specific
- Flexibility, the defined function module should have the least function, which makes the module adapt the unpredictability and tolerant to modification
- Brevity, the control system should have a definite manipulation, avoid unnecessary complexity
- Easy to operate, has a good communication interface, the defined interface module, the path planning and the necessary control command should be simple

Structure of distributed driving based on CAN bus: Motor driver based on CAN bus takes TI Corporation's TMS320LF2407A DSP chip as control core and it uses LMD18200 as power amplifier to drive DC motor and uses relay to control brake of motor. Data exchanging between main computer and driver is through CAN interface. Control mode of steering wheel and driving wheel is different: Driven steering wheel can realize closed position control by angle sensor on the basis of speed loop. Its structure is shown in Fig. 4.

Three simple driving modes are integrated in motion driver of distributed network:

- Encoder speed control mode, wheel speed can keeps invariant with no regard of the terrain condition
- Current control mode, under this control mode, the output torque of every wheel is constant regardless of the terrain

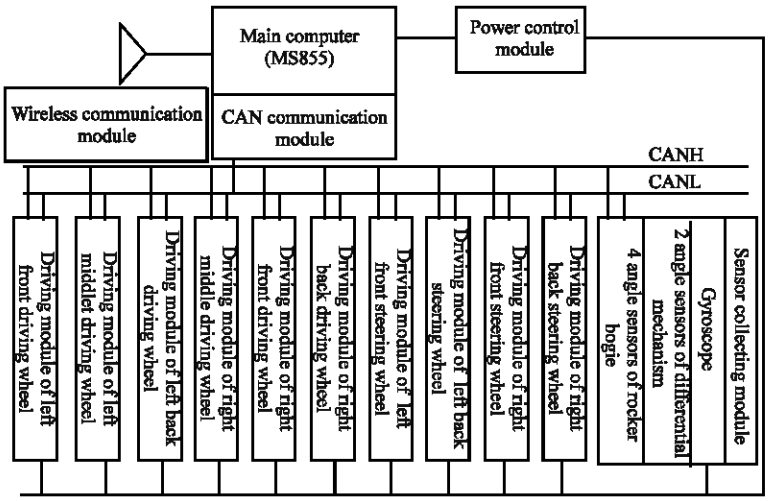

Fig. 2: Distributed network control diagram of rover' control system

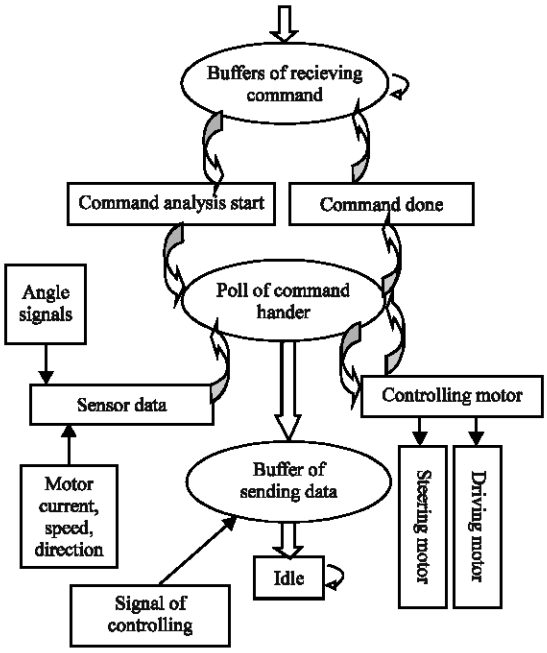

Fig. 3: Software structure of mobile system of lunar rover

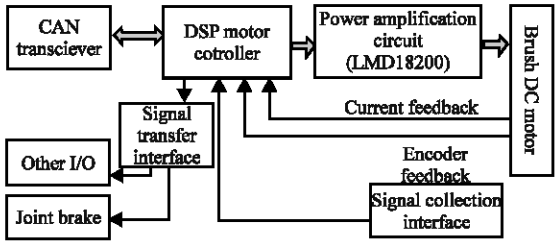

Fig. 4: Principle diagram of distributed motion driver

- I×R compensation mode, when operating at slow speeds, the mechanical load on the motor being driven is monitored and compensated when necessary, by an automatic increase in output voltage to maintain constant speed. This occurs for heavy or uneven loads (e.g., the Yoyo effect which has greater resistance during its upward travel)

KINEMATICS MODEL OF ROVER

To the smooth wheel and wheel with grouser of 5, 10 and 15 mm height respectively, the results of DP and T at different grouser spacing for various wheel slip were shown in Fig. 3. When rover moves in straight line on plane, its speed can be guaranteed with inputting each wheel same speed. But in order to steer no slip, its steering kinematics must be made according to steering requirement. The analysis of kinematics is followed as.

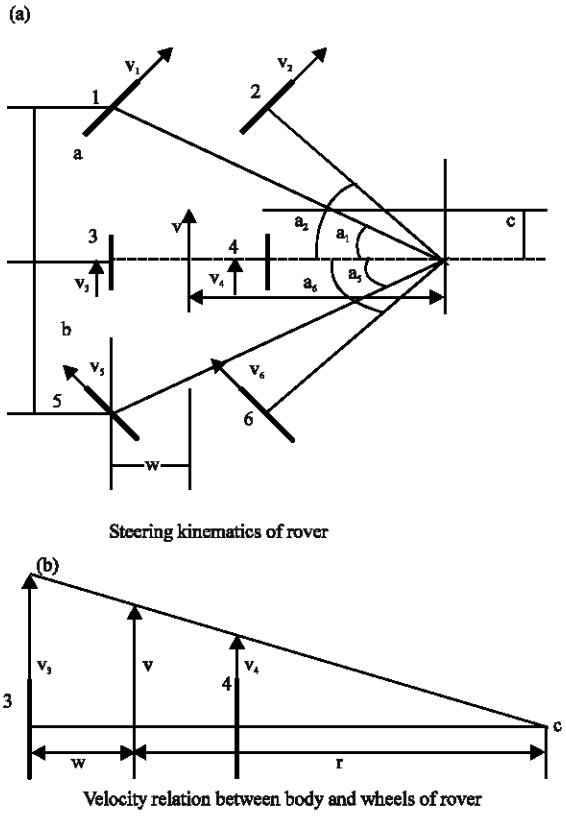

Fig. 5: Steering kinematics of rover and velocity relation between body and wheels of rover

The kinematics of steering is shown in Fig. 5. From this, relation between angle of steering wheel and configuration dimension of rover can be made:

$$\left.\begin{aligned}\alpha_1 = a\tan(a/(r+w)), \alpha_2 = a\tan(a/(r-w))\\ \alpha_5 = -a\tan(b/(r+w)), \alpha_6 = -a\tan(b/(r-w))\end{aligned}\right\} \quad (1)$$

where, w is half of distance between two wheels; a is distance between centre of rover body and centre of front steering wheel; b is distance between centre of rover body and centre of back steering wheel, r is distance between centre of rover body and turning centre; α_1, α_2, α_3, α_4, α_5, α_6 is angle of steering wheel, respectively and it is defined that counter-clockwise steering angle values is positive and vice versa and r value is positive in the right of rover body' centre line and vice versa. From Fig. 5a, r, α_5 and α_6 is positive, α_1 and α_2 is negative and α_3, α_4 is zero.

From Fig. 5b, relation between speed of driving wheel and configuration dimension can be obtained:

$$v_3 = v\times(w-r)/r, \quad v_4 = v\times(w+r)/r \quad (2)$$

where, v_3 is speed of left middle wheel, v_4 is speed of right middle wheel.

According to steering speed of each wheel which is relative to turning centre C, following equations can be given:

$$v_i / r_i = v_{middle} / r_{middle}, \quad r_i / r_{middle} = 1/\cos\alpha_i \tag{3}$$

Relations between speed of other driving wheel and configuration dimension of rover are followed as:

$$\left.\begin{array}{l} v_1 = v_3 / \cos\alpha_1, v_2 = v_4 / \cos\alpha_2 \\ v_5 = v_3 / \cos\alpha_5, v_6 = v_4 / \cos\alpha_6 \end{array}\right\} \tag{4}$$

where, v_1 is speed of left front wheel, v_2 is speed of right front wheel, v_5 is speed of left back wheel, v_6 is speed of left back wheel.

When rover turns in place, speed of its steering wheel can be deduced from letting be r = 0 in Eq. 1-4 and speed of its driving wheel can be deduced from turning speed of rover body (ω_{body}). The equations are as followed:

$$\left.\begin{array}{r} v_1 = \pm\omega_{body} \times \sqrt{a^2 + w^2}, v_2 = m\omega_{body} \times \sqrt{a^2 + w^2} \\ v_3 = \pm\omega_{body} \times w, v_4 = m\omega_{body} \times w \\ v_5 = \pm\omega_{body} \times \sqrt{b^2 + w^2}, v_6 = m\omega_{body} \times \sqrt{b^2 + w^2} \end{array}\right\} \tag{5}$$

RESEARCH ON MOTION CONTROL OF ROVER

The control strategy of rover's locomotion is shown in Fig. 6. Main computer receives command form remote console and uses kinematics model and control algorithm to send command to each networking driver, then driver implement task according to command received. Firstly, wheel motion mode is analyzed.

Analysis of wheels operational mode: In case of general rover motions, the operation of wheel is characterized by individual speed and force parameters. Force and torques are exerted on wheels and the values of their longitudinal and lateral slipping are different and are determined by the operational conditions of each wheel. Let one wheel as researching, scheme of analysis of force acting on wheel is shown in Fig. 7. In the scheme the relationship between the wheel and the driving, the soil surface and frame are represented by the corresponding forces. M_{ki} is the torque from the driving acting on the i-th wheel unit (related to unit contact area). q_{ni} is the normal reactions of the soil; q_{ti} is the tangential reactions of soil; $q_{\mu i}$ is the lateral reactions of the soil. The resultant of all these forces acting on the wheel (the resultant force) is Pi. The projections of the resultant Pi defined at the wheel axis are indicated by P_{xi}, P_{yi} and P_{zi}.

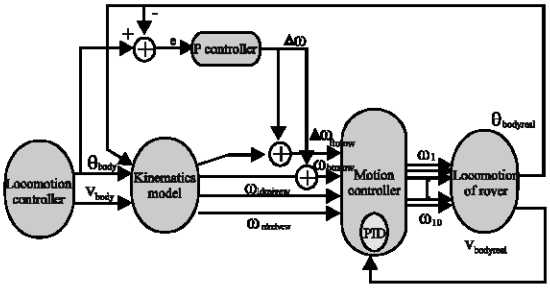

Fig. 6: Whole control model of mobile system

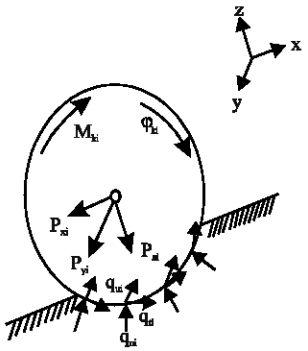

Fig. 7: Force analysis of independent driven wheel

In case of general rover motions, the operation of wheel is characterized by individual speed and force parameters. Force and torques are exerted on wheels and the values of their longitudinal and lateral slipping are different and are determined by the operational conditions of each wheel. Let one wheel as researching, scheme of analysis of force acting on wheel is shown in Fig. 7. In the scheme the relationship between the wheel and the driving, the soil surface and frame are represented by the corresponding forces. M_{ki} is the torque from the driving acting on the ith wheel unit (related to unit contact area). q_{ni} is the normal reactions of the soil; q_{ti} is the tangential reactions of soil; $q_{\mu i}$ is the lateral reactions of the soil. The resultant of all these forces acting on the wheel (the resultant force) is P_i. The projections of the resultant P_i defined at the wheel axis are indicated by P_{xi}, P_{yi} and P_{zi}.

For detailed or more advanced analysis, we introduce concept of operation mode of wheel. The operation mode of wheel is the state of wheel of rover from the angle of the mechanics and driving when rover is moving. As applied to analysis operation mode of wheel, the projection of the resultant force to the x-axis is of major important. It allows judging mutual influences on the wheels a multi-driving rover and estimate value and pattern of distributed force flows. Obviously, when $P_{xi} = 0$, there is no mutual influences on wheels; when $P_{xi} \neq 0$, the considered wheel either shifts a part of its

force to other wheels (push-wheel) or on the contrary, requires push force for its motion from the rover (pushed wheel). These considerations lead to classifying the operational modes of a rover wheel. The following operational modes can be defined: (1) driving mode, pushing wheel: $P_{xi}<0$, $M_{ki}>0$, (2) driving mode, pushed wheel: $P_{xi}>0$, $M_{ki}>0$, (3) driven mode: $P_{xi}>0$, $M_{ki} = 0$, (4) braking mode: $P_{xi}>0$, $M_{ki} = 0$ and (5) free running mode: $P_{xi} = 0$, $M_{ki}>0$. Thereinto, the P_{xi} sign is in relation to the x-coordinate (rover forward direction) and the M_{ki} sign is in relation to the $\dot{\varphi}_{ki}$.

We may obtain from the wheel operation mode: As to the lunar rover driven by multi wheels, if some wheels are under driving mode and they themselves are driving wheels, there must be wheels which are under driving mode as driven wheels or wheels under driven mode, vice versa. If some wheels are under driving pattern or driven pattern, action and reacting force must exist, inevitably leading to energy loss. While the wheels are under free mode, there is no action and reacting force, so that no energy loss is caused by un-matching velocity of multi-wheel drive in the mechanism.

Simple control modes based on bus drivers: As a multi-driving rover, the accepted physical prerequisite means, among other factors, that at any arbitrary moment of time each wheel or any group of wheels of a lunar rover can work in any of the modes mentioned above. There can be found both open loop force flux (passive) through soil, wheels and the frame and closed loop force flux (active) driven by the on-board power source including some energy reflection or recovery into the power supply network. To begin with, the influence on mechanism driving under the simple control modes is analyzed.

With each wheel having the same initial velocity, we found by experiment that in flat terrain, the lunar rover in the above three modes has the same basic results, each wheel's electrical current feedback agreeing roughly, $P_{xi}=0$, $M_{ki}>0$, indicating that the reacting force among wheels is zero and every wheel is under free rolling mode. While, the rover is in rough terrain, there is great difference among the output results of the three control patters.

- Under encoder speed control mode, the force of the bogie point is obviously larger than that of the other two modes and the wheels are easy to slip. Obviously, the reacting forces of bogie point increase and we know that wheels are under un-free mode, i.e., $P_{xi} \neq 0$. (When the equivalent force reacted by the forward wheels is greater than that reacted by the backward wheels, $P_{xi}>0$ and on the contrary, $P_{xi}<0$)
- Under compensation mode, the moving velocity of lunar rover can be controlled and the wheel slipping will decrease, but there is still some force at mast place
- Under current control mode, wheel slipping decrease obviously as well as the force at bogie point, but the velocity is not under control, i.e., a certain output condition given, the velocity will change if the terrain condition changes. Obviously, P_{xi} is approximately zero at the third condition and every wheel of lunar rover is under free operation pattern. Among of parts of lunar rover there are not mutual influences

Improved control algorithm: In order to solve phenomenon above, motion model of rover is made in rough terrain. In Fig. 8 coordinate system XYZ is coordinate system of one side of rover suspension (XZ is motion plane of rover). θ_i is contact angle between wheel and terrain on ith wheel. α and ρ are respectively angle between rocker-bogie and horizontal plane. v_1, v_2 and v_3 are, respectively speed of wheel centre in side of suspension.

From Fig. 8, if 3 linear velocity of wheel are same, their projection vector in plane XZ will be different. When rover moves in rough terrain, if each given reference speed of wheel is equal, some wheels will slip, leading to increased energy consumption and declined climbing ability. Therefore, we can use the method of compensation to match driving velocity of each wheel. For each wheel, the angle between its linear speed and the terrain has to be taken into account to prevent slippages. The matching condition of wheels at the same side of the

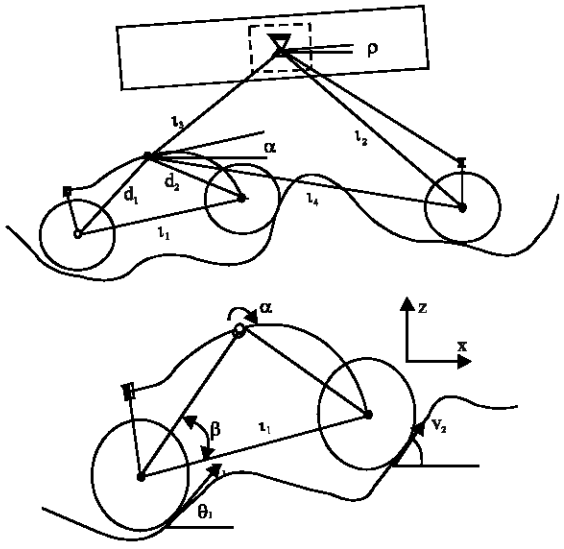

Fig. 8: Speed of wheels analysis in rough terrain

rover is $v_1\cos\theta_1 = v_2\cos\theta_2 = v_3\cos\theta_3$. For convenience of research, this method assumes that each wheel has a single point of contact with a smooth terrain. We also assume non-deformable terrain and that all wheels are in contact with the terrain. From fig. 8, we can obtain equations (Iagnemma and Dubowsky, 2000):

$$v_1\cos(\theta_1-\alpha) = v_2\cos(\theta_2-\alpha) \quad (6)$$

$$v_2\sin(\theta_2-\alpha) - v_1\sin(\theta_1-\alpha) = l\dot{\alpha} \quad (7)$$

If v_1, v_2 is given, from (1) and (2), estimation of contact angle is as follows:

$$\theta_1 = \alpha - q_1\cos q_2 \quad (8)$$

$$\theta_2 = q_1\cos(q_3/q_2) + \alpha \quad (9)$$

Where:

$q_3 = \frac{1}{2q_1}\sqrt{2q_1^{\,2} + 2q_2^{\,2} + 2q_1^{\,2}q_2^{\,2} - q_1^{\,4} - q_2^{\,4} - 1}$

$q_1 = l\dot{\alpha}/v_1$

$q_2 = v_2/v_1$

Analysis of speed and contract angle of back wheel is shown in Fig. 9, where, C_L is bogie's instantaneous centre of velocity, R_{fL}, R_{mL}, R_{BL}, respectively is instantaneous radius of front wheel, middle wheel and bogie point. From Fig. 9, we can obtain:

$$\theta_3 = \arccos\left[\frac{v_{BogieL}}{v_3}\cos(\alpha-\rho)\right] \quad (10)$$

Where:

$$v_{BogieL} = \dot{\alpha}R_{BL}$$

$$R_{mL} = \frac{l_1\sin(\pi/2-(\theta_1-\rho)}{\sin(\theta_1-\theta_2)}$$

$$R_{BL} = \sqrt{d_1^2 + R_{mL}^2 - 2d_1R_{mL}\cos(\frac{\pi}{2}+\theta_2-\rho-\beta)}$$

According to the given analysis, if that condition is respected at any time, this method should not induce any slipping situation. Obviously, this does not mean that no slippage will ever actually occur, but the application of this method will reduce them significantly.

Improved control algorithm is constructed by principle of velocity matching above. Through real-time measurement of rover's pose and wheels speed, estimation of contract angle is computed to regulate the speed of each wheel, to reduce slipping on rough terrain. Implementation of improved control algorithm is as follows:

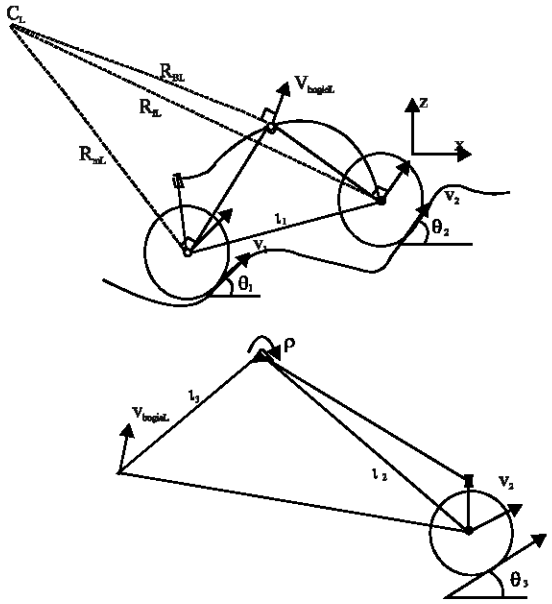

Fig. 9: Contract speed analysis back wheel in rough terrain

- Firstly assumes wheels are not slipping. Speed of each wheel requires $v_i = v_{body}$ (I = 1, 2..., 6)
- According to equations (8), (9) and (10), computes contract angle between wheel and terrain θ_i
- Computes $v_{ix} = v_i\cos\theta_i$ and $\Delta v_i = |v_{body} - v_{ix}|$
- If $\Delta v_i \le \delta$ (δ is given Allowable Value of error), then implements (2)-(4) if, $\Delta v_i \le \delta$, judges whose speed v_{ix} is exceed δ, then let $v_i = v_i + \Delta v$ (Δv is velocity increment), continues to implement (2)-(4) till $\Delta v_i \le \delta$

Preliminary test shows energy consumption can be decreased after above method is adopted. When rover with rocker-bogie moves in sandy rough terrain, given same time, moving distance using improved control algorithm increased by 5% compared to using speed control mode and currents of wheels are decreased by 4% (Fig. 14).

EXPERIMENTS

In order to verify performances of locomotion, networking drivers based on CAN bus and whole control system, experiments such as obstacle overcoming, climbing, moving on cross-hill in soft soil and spot turning are implemented, results are shown in Fig. 10-13.

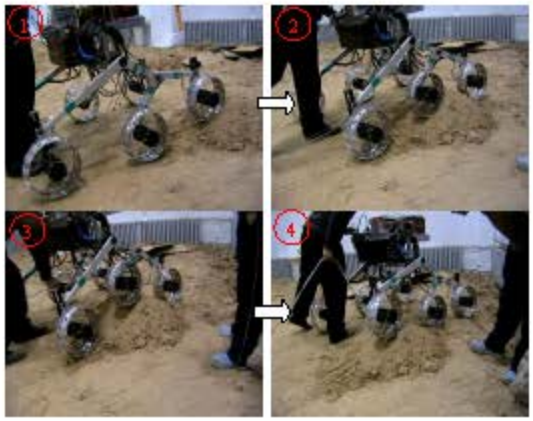

Fig. 10: Obstacle overcoming testing

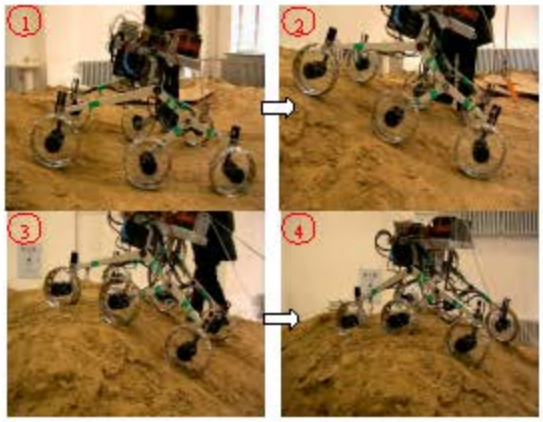

Fig. 11: Climbing testing in soft soil

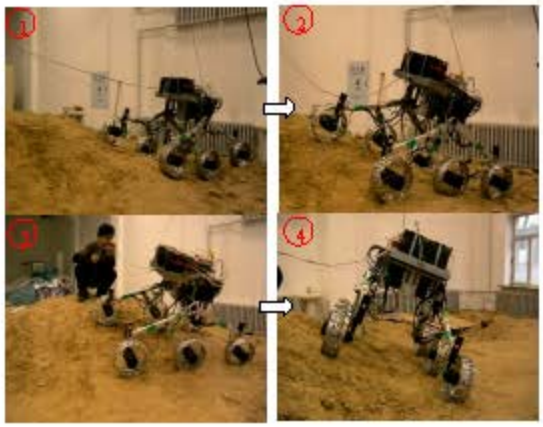

Fig. 12: Moving testing on cross-hill slope

Figure 10 is progress of overcoming obstacles of single side of rover. In this experiment, high of obstacle is 250 mm. In Fig. 10 (1-3), respectively are states of front wheel, middle wheel and back wheel overcoming obstacle.

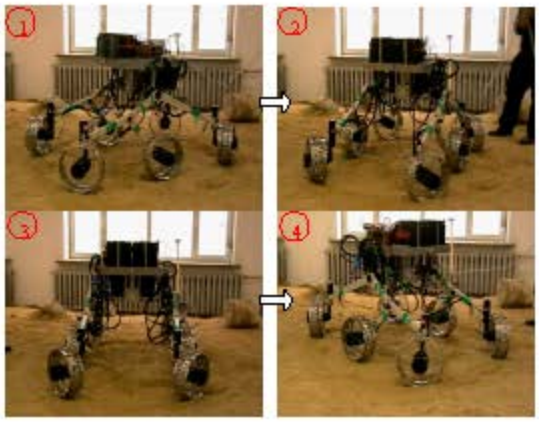

Fig. 13: Spot turn testing

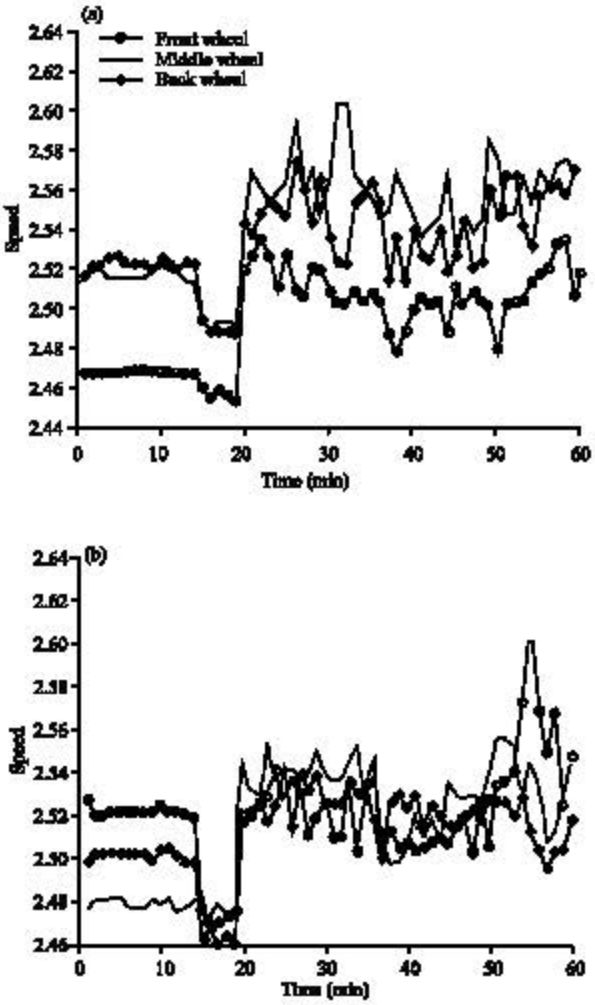

Fig. 14: Compare of wheel' driving current under different control methods on rough slope terrani. (a) Encoder speed control mode and (b) Improved control mode

Results shows suspension of rover with rocker bogie and drivers can satisfy design requirements.

Figure 11 is progress of climbing in sandy terrain. Experiments shows rover's maximum climbing in sandy terrain is 28 degrees and contrast experiment of different configuration of wheel shows that Elastic sieve wheel can be more suitable in sandy terrain and it can improve performance of driving.

Figure 12 is progress of moving testing on cross-hill slope in sandy terrain. In this experiment, slop is 28 degrees. Results show that rover has good anti roll ability and stability to move in rough terrain.

Figure 13 is progress of turning in place in sandy terrain. According to turning kinematics above, rover can realize turning in place. Results show turning kinematics is correct and performance of drivers base CAN bus is good.

In order to verify performance of improved control algorithm, experiments between simple basic control mode and improved control mode are made on rough terrain. Results are shown in Fig. 10. Figure 14a is driving current of wheels in left side of rover under simple encoder speed control mode and Fig. 14b is driving current of wheels in left side of rover under improved control algorithm. Results show that driving currents under simple speed mode is more than driving currents under improved control mode, especially driving current of back wheel, it is decreased by about 4%.

CONCLUSIONS

Control system of rover with digital servo technology based on CAN bus has characteristics of simple structure, high precision, high reliability and takes up few system resources. Distributed control structure based CAN bus increases software efficiency and improves real-time of system. Reasons of energy consumption and advantages and disadvantages, respectively of simple control modes are analyzed through experiments. Based on configuration of rover's suspension and principle of velocity matching, improved control algorithm is presented, experiments results show that this method can improve motion performance of locomotion, decrease slip of wheel and energy consumption in sandy rough terrain. At last, through the experiments of obstacle overcoming, climbing, moving on cross-hill in soft soil and spot turning, it shows this robot has good transportation performance and the distributed motion control system base CAN bus has a good performance and high reliability.

ACKNOWLEDGMENTS

This research was supported by National High Technology Research and Development Plan of China (Grant No. 2006AA04Z231), Natural Science Foundation of Heilongjiang Province of China (Grant No. ZJG0709) and The 111 Project (Grant No. B07018).

REFERENCES

Chen, X.F., Z.B. Shu and Y.K. Zhao, 2006. Study and application of motion control system based on multi-servo control mode. Micromotors, 39: 45-48.

Iagnemma, K., R. Burn, E. Wilhelm and S. Dubowsky, 1999. Experimental validation of physics-based planning and control algorithms for planetary robotic rovers. Proceedings of the 6th International Symposium on Experimental Robotics, May 01, Sydney, Australia, pp: 319-328.

Iagnemma, K. and S. Dubowsky, 2000. Vehicle wheel-ground contact angle estimation: With application to mobile robot traction control. Proceedings of the 7th International Symposium on Advances in Robot Kinematics, July 2000, Cambridge, MA USA., pp: 137-146.

Lin, M., J.H. Zhu, J.H. Meng and S. Zengqi, 2002. Tsinghua lunar rover prototype and its hardware design. Proc. IEEE/TENCON, 3: 1578-1581.

Matijevic, J. and D. Shirley, 1997. The mission and operation of the mars pathfinder microrover. Control Eng. Pract., 5: 827-835.

Nesnas, I.A., A. Wright, M. Bajracharya, R. Simmons, T. Estlin and W.S. Kim, 2003. CLARAty: An architecture for reusable robotic software. Proceedings of the SPIE's AeroSense Symposium, 2003, Florida, USA., pp: 253-264.

Schenker, P.S., E.T. Baumgartner, P.G. Backes, H. Aghazarian and L.I. Dorsky *et al*., 2001. FIDO: A field integrated design and operations rover for mars surface exploration. Proceedings of the 6th International Symposium on Artificial Intelligence, May 21, Robotics and Automation in Space, Montréal, Canada, pp: 1-8.

Volpe, R., I. Nesnas, T. Estlin, D. Mutz, R. Petras and H. Das, 2001. The CLARAty architecture for robotic autonomy. Proceedings of IEEE Aerospace Conference, March 10-17, California, USA., pp: 1121-1132.